

# **Ly $\alpha$ line formation in starbursting galaxies**

## **II. Extremely Thick, Dustless, and Static HI Media**

Sang-Hyeon Ahn

*Korea Institute for Advanced Study, 207-43 Cheongyangri-dong, Dongdaemun-gu, Seoul, 130-012, Korea*

sha@kias.re.kr

Hee-Won Lee

*Department of Earth Science, Sejong University, Seoul 143-747, Korea*

and

Hyung Mok Lee

*School of Earth and Environmental Sciences, Astronomy Program, Seoul National University, Seoul 151-742, Korea.*

### **ABSTRACT**

The Ly $\alpha$  line transfer in an extremely thick medium of neutral hydrogen is investigated by adopting an accelerating scheme in our Monte Carlo code to skip a large number of core or resonant scatterings. This scheme reduces computing time significantly with no sacrifice in the accuracy of the results. We applied this numerical method to the Ly $\alpha$  transfer in a static, uniform, dustless, and plane-parallel medium. Two types of photon sources have been considered, the midplane source and the uniformly distributed sources. The emergent profiles show double peaks and absorption trough at the line-center. We compared our results with the analytic solutions derived by previous researchers, and confirmed that both solutions are in good agreement with each other. We investigated the directionality of the emergent Ly $\alpha$  photons and found that limb brightening is observed in slightly thick media while limb darkening appears in extremely thick media. The behavior of the directionality is noted to follow that of the Thomson scattered radiation in electron clouds, because both Ly $\alpha$  wing scattering and Thomson scattering share the same Rayleigh scattering phase function. The mean number of wing scatterings just before escape is in exact agreement with the prediction of the diffusion approximation. The Ly $\alpha$  photons constituting

the inner part of the emergent profiles follow the relationship derived from the diffusion approximation. We present a brief discussion on the application of our results to the formation of Ly $\alpha$  broad absorption troughs and P-Cygni type Ly $\alpha$  profiles seen in the UV spectra of starburst galaxies.

*Subject headings:* line: formation — radiative transfer — galaxies: starburst — galaxy: formation

## 1. Introduction

Recent observational achievements in spectroscopy of galaxies in the very early universe (Steidel et al. 1996, 1999) have enabled us to study starburst galaxies whose star formation rates are very high. Since these galaxies are at  $3 < z < 5$ , we can observe their ultraviolet continua and Ly $\alpha$  in the optical band, which can be covered by ground-based large telescopes. Furthermore, Ly $\alpha$  is one of the most conspicuous emission lines, and the investigation of the Ly $\alpha$  line transfer becomes important in understanding the physical nature of these galaxies.

The Ly $\alpha$  profiles of many starburst galaxies in the early universe are categorized into three types : symmetric Ly $\alpha$  emission, asymmetric or P-Cygni type one, and broad absorption in damping wings (Tenorio-Tagle et al. 1999). Moreover, local starburst galaxies also show similar characteristics (Kunth et al. 1998). The P-Cygni type Ly $\alpha$  is believed to originate from the expanding neutral medium surrounding the Ly $\alpha$  source, which is supported by the existence of the low ionization interstellar absorption lines blueshifted relative to the line-center (Kunth et al. 1998; Lee & Ahn 1998; Ahn et al. 2000). The Voigt profile fittings for the broad absorption lines extending to the Lorentzian wings and P-Cygni type absorption lines revealed that their neutral hydrogen column density  $N_{\text{HI}} = 10^{19} - 10^{22} \text{ cm}^{-2}$  or the line-center optical depth  $\tau_0 = 10^6 - 10^9$ . However, the Voigt profile fitting is not satisfactory in the red part of Ly $\alpha$  emission which is thought to be contributed by back-scattered photons. This is exemplified by the ill-fitted red part of Ly $\alpha$  emission in the spectrum of Haro 2 (Legrand et al. 1997). No adequate computational method to describe the back-scattered photons has been developed so far.

In extremely thick media of hydrogen, where Ly $\alpha$  photons wander in both real space and frequency space, the line transfer can be described by the diffusion approximation. In the diffusion approximation we assume that only wing scatterings play a significant role in transferring Ly $\alpha$  photons in space. However, this approximation does not fully take into account the fact that the photons move back and forth between core and wing wavelength regimes during their transfer in an extremely thick medium. While being a core photon the

scatterings are resonant and therefore local. Wing scatterings are associated with significant spatial excursion. Furthermore, the scattering phase functions for resonant scatterings associated with the  $S_{\frac{1}{2}} \rightarrow P_{\frac{1}{2},\frac{3}{2}}$  transitions are different from that associated with wing scatterings which is identical with that of the classical Rayleigh scattering. This fact should be considered in a very careful manner in computing the physical quantities such as the polarization and the angular distribution of the emergent radiation field.

In this paper, we investigate the Ly $\alpha$  line transfer in an extremely thick and static medium by using a Monte Carlo method. We will focus only on the dustless case in this work, even though the dusty case is more realistic. The effect of dust was briefly dealt by Ahn et al. (2000) and more careful investigation is deferred. Our assumption can be valid for the primeval objects that had not experienced any star-formation episode.

This is the second paper in a series on the Ly $\alpha$  profile formation in starbursting galaxies. In the first paper (Ahn et al. 2001) we studied the Ly $\alpha$  transfer in moderately thick media. We use the Monte Carlo method, which is frequently adopted in the Ly $\alpha$  line transfer, because of its simplicity and flexibility. However, the Monte Carlo method becomes inefficient when the line-center optical depth  $\tau_0$  of scattering medium is very large. We need to follow the scattering of each photon until the escape, and the number of scattering is proportional to  $\tau_0$  for very thick case. This means that the number of computations grows in proportional to  $\tau_0$  which could vary by several orders of magnitudes depending on the situation. Our previous version of the code consumes unacceptably long computing time for extremely thick cases. We therefore extend our efforts to very large optical depth regime in this paper by developing the ‘accelerating scheme’.

This paper is composed as follows. In section 2, we describe our scheme to accelerate the Monte Carlo code. In section 3 we show our results. In section 4 we discuss possible applications of our code. The final section summarizes our major findings.

## 2. Configuration and Monte Carlo Method

Since we are interested in the emergent Ly $\alpha$  profiles in various situations, we first introduce the dimensionless parameter  $x$  defined by

$$x \equiv \Delta\nu/\Delta\nu_D = (\nu - \nu_0)/\Delta\nu_D, \quad (1)$$

which describes the frequency shift from the line-center  $\nu_0$  in units of the Doppler shift  $\Delta\nu_D \equiv \nu_0(v_{th}/c)$ . Here  $v_{th}$  is the thermal speed of the scattering medium,  $c$  is the speed of light, and  $\nu_0$  is the line-center frequency.

The medium considered in this study is a plane-parallel slab, which is uniformly filled

with pure hydrogen atoms. The optical depth at the Ly $\alpha$  line-center from the center to both sides of the medium along the normal direction is  $\tau_0$ . We consider two types of the source distribution: a source in the midplane, and sources uniformly distributed along the vertical line. We show the configuration considered in this study in Figure 1. The underlying ideas for these two cases is that the midplane source can model a giant H II region embedded in a neutral region while the uniformly distributed source can mimic the starbursting region which has young stars mixed with the partially ionized gas. These configurations are the same ones that have been considered in the previous works (Neufeld 1990; Adams 1972).

There have been several Monte Carlo approaches to the resonance line transfer in an optically thick and static medium in the literature (Avery & House 1968; Adams 1972; Meier & Lee 1981; Gould & Weinberg 1996). The main advantages of Monte Carlo methods lie in the geometrical flexibility of scattering media and the simplicity in solving the radiative transfer problem, compared with the direct numerical integration of the basic radiative transfer equation. However, one severe limitation of the technique is that a large amount of computing time is required for the cases with extremely high optical depths. In order to handle the Ly $\alpha$  transfer for extremely large  $\tau_0$  using currently available computers, we modified the prototypical Monte Carlo code developed in our previous papers (Ahn et al. 2000, 2001).

### 2.1. Acceleration Scheme for Extremely Thick Medium

As was shown numerically in the previous papers (Ahn et al. 2000, 2001) and explained in accordance with Adams (1972), in extremely thick media, Ly $\alpha$  photons escape from the media by both frequency diffusion and spatial diffusion. When a Ly $\alpha$  photon is emitted with the line center frequency in an optically thick medium, then it experiences a large number of core scatterings. During the core scatterings, the photon does not move much because the line-center opacity is very large. During a series of a large number of core scatterings, the Ly $\alpha$  photon can be scattered by a rapidly moving atom in the tail of the Maxwell-Boltzmann velocity distribution. Once the photon is scattered by such an atom, its frequency changes abruptly and it becomes a wing photon. For a wing photon, the hydrogen medium becomes more transparent and the photon traverses a longer distance. In a moderately thick medium with  $10^3 < \tau_0 < 10^3/a$ , where  $a$  is the Voigt parameter, Ly $\alpha$  photons escape from the medium during at most a few wing scatterings; but in extremely thick media with  $a\tau_0 > 10^3$ , the wing photon can not escape and have to experience a number of continuous wing scatterings, whose number is approximately given by  $\langle N \rangle = x_s^2$  assuming random walk approximation (Adams 1972). Here  $x_s = (a\tau_0)^{1/3}$  is the frequency at the peaks of profiles.

During such wing scatterings some photons become core photons again by the so called ‘restoring force’ (Adams 1972), and then these photons suffer a large number of successive core scatterings. One cycle of these processes is called ‘an excursion’ (Adams 1972), and the photon spatially transfers by the repetition of excursions before it eventually achieves its escape from the medium during the wing scatterings: this final step of escape is called ‘single longest excursion’.

Considering these transfer processes, we can see that the major consumption of time in the Monte Carlo code occurs in the step of the computation of the outgoing wavevector associated with resonant or core scatterings, whose number of successive core scattering is order of  $\tau_0^2$ . Therefore, the computing time can be significantly saved if we simplify this step in a clever way. Our code was developed to distinguish the resonant core scattering from the non-resonant wing scattering. Thus, in order to save the computing time, whenever the photon experiences a resonant scattering during its transfer, we can skip following successive resonant scatterings and to describe the next scattering by a fast moving hydrogen atom.

We now explain the skipping procedure in detail. The main idea for the procedure is to assume that any photons with  $|x_1| < x_c$  suffer a large number of core scatterings locally and finally emerges from the local scattering region with frequency shift  $|x_2| > x_c$  after a scattering with a rapidly moving atom, where  $x_c$  is the critical frequency shift which defines the borderline between core and wing photons. In the accelerating scheme, we just skip the core scatterings and assigns  $x_2$  in an appropriate way. For the Lorentzian profile of Ly $\alpha$  scattering,  $x_c$  can be safely set to  $0 < x_c \leq \sqrt{\pi}$  for moderately thick media with  $10^3 < \tau_0 < 10^3/a$ , and to  $x_c = \sqrt{\pi}$  for extremely thick media with  $a\tau_0 > 10^3$ . Here we obtain  $\sqrt{\pi}$  from the Eq. (10) by substituting the effective wing optical depth  $\tau_w = 1$ . We find that the slightly larger  $x_c$  can be permitted for even larger  $\tau_0$ .

In order to describe the scattering by a fast moving atom, we select the velocity ( $v$ ) of the scattering atom from the volcano-type thermal velocity distribution (Avery & House 1968)

$$P(v) = \frac{1}{\sqrt{\pi}} \exp(-v^2), \quad (2)$$

where  $x_c \leq v \leq v_{max}$ , rather than from a simple Gaussian distribution. Here  $v_{max}$  is safely set to be as large as  $v_{max} = 10$ . We call this method ‘the accelerating scheme’. We note that this method is valid for  $a\tau_0 \ll 10^3$  only when  $x_c \rightarrow 0$ , which is tantamount to restoring the original code.

## 2.2. Angular Redistribution and Polarization

In this subsection, we provide the details of the angular redistribution and polarization of the scattered radiation. Our code treats the scattering of Ly $\alpha$  photons in a manner very faithful to the atomic physics associated with the fine structure of hydrogen. The level splitting of  ${}^2P_{\frac{1}{2},\frac{3}{2}}$ , the excited state of Ly $\alpha$  transition, is 10GHz, which amounts to the Doppler width of 1.3 km s $^{-1}$ . Because this is much smaller than the thermal speed in a medium with  $T \geq 100$  K, one normally neglect the  ${}^2P_{\frac{1}{2},\frac{3}{2}}$  level splitting, treating it as a single level. However, even though  $T < 100$  K, the level splitting can be negligible when the medium has a large optical thickness.

As is described in Ahn et al. (2000, 2001), in our Monte Carlo code we compute the probability that the given photon is resonantly scattered with one of the two levels  $P_{\frac{1}{2},\frac{3}{2}}$  and the probability that the scattering occurs in the damping wings at each scattering event. We adopt the density matrix formalism to describe the angular distribution and polarization of the scattered Ly $\alpha$ , where the density operator is represented by a  $2 \times 2$  Hermitian matrix. The density matrix element associated with the scattered photon  $\rho_{\beta\beta'}$  is related with that of the incident photon  $\rho_{\alpha\alpha'}$  by

$$\rho_{\beta\beta'} \propto \sum_{I,I'=P_{3/2},P_{1/2},\alpha,\alpha'} \frac{(\hat{\mathbf{r}} \cdot \boldsymbol{\epsilon}^{(\beta')})_{AI} (\hat{\mathbf{r}} \cdot \boldsymbol{\epsilon}^{(\alpha)})_{IA}}{E_I - E_A - \hbar\omega} \rho_{\alpha\alpha'} \frac{(\hat{\mathbf{r}} \cdot \boldsymbol{\epsilon}^{(\alpha')})_{I'A}^* (\hat{\mathbf{r}} \cdot \boldsymbol{\epsilon}^{(\beta)})_{AI'}^*}{E_{I'} - E_A - \hbar\omega}. \quad (3)$$

Here, the matrix elements due to other  $nP(n > 2)$  terms are neglected, and the radial part of the matrix elements  $\langle 2p || r || 1s \rangle$  is treated as a constant. The relevant Clebsch-Gordan coefficients are found in Condon & Shortley (1951); Lee et al. (1994).

As is shown by Stenflo (1980), scattering of Ly $\alpha$  in the damping wings is characterized by the classical Rayleigh scattering phase function due to the quantum interference between the two levels  $P_{\frac{1}{2},\frac{3}{2}}$ . In this case, one can show that the Ly $\alpha$  scattering in the wings can be regarded as a resonance scattering between two levels with  $J = 0$  and  $J = 1$  as far as the scattering phase function is concerned. The computation of the matrix elements in this case is straightforward and the result is

$$\begin{aligned} \rho'_{11} &= \cos^2 \Delta\phi \rho_{11} - \cos \theta \sin 2\Delta\phi \rho_{12} + \cos^2 \theta \sin^2 \Delta\phi \rho_{22} \\ \rho'_{12} &= \frac{1}{2} \cos \theta' \sin 2\Delta\phi \rho_{11} + (\cos \theta \cos \theta' \cos 2\Delta\phi + \sin \theta \sin \theta' \cos \Delta\phi) \rho_{12} \\ &\quad - \cos \theta (\sin \theta \sin \theta' \sin \Delta\phi + \frac{1}{2} \cos \theta \cos \theta' \sin 2\Delta\phi) \rho_{22} \\ \rho'_{22} &= \cos^2 \theta' \sin^2 \Delta\phi \rho_{11} + \cos \theta' (2 \sin \theta \sin \theta' \sin \Delta\phi + \cos \theta \cos \theta' \sin 2\Delta\phi) \rho_{12} \\ &\quad + (\cos \theta \cos \theta' \cos \Delta\phi + \sin \theta \sin \theta')^2 \rho_{22}, \end{aligned} \quad (4)$$

where the incident radiation is characterized by the wavevector  $\hat{\mathbf{k}}_i = (\sin \theta \cos \phi, \sin \theta \sin \phi, \cos \theta)$  and the outgoing wavevector  $\hat{\mathbf{k}}_f$  is correspondingly given with angles  $\theta'$  and  $\phi'$  with  $\Delta\phi = \phi' - \phi$ . Here, we assume that the circular polarization is always zero due to the azimuthal symmetry in the scattering geometry and initial condition.

In the case of resonance scattering between  $J = \frac{1}{2}$  and  $J = \frac{3}{2}$  levels, a straightforward calculation shows that the density matrix elements associated with the outgoing photons are given by

$$\begin{aligned}
 \rho'_{11} &= (5 + 3 \cos 2\Delta\phi)\rho_{11} \\
 &\quad + [(5 - 3 \cos 2\Delta\phi) \cos^2 \theta + 2 \sin^2 \theta]\rho_{22} - 6 \cos \theta \sin 2\Delta\phi \rho_{12} \\
 \rho'_{12} &= 3 \sin 2\Delta\phi \cos \theta' \rho_{11} + 6(\cos \theta \cos \theta' \cos 2\Delta\phi + \sin \theta \sin \theta' \cos \Delta\phi)\rho_{12} \\
 &\quad + 3 \cos \theta(-2 \sin \theta \sin \theta' \sin \Delta\phi - \cos \theta \cos \theta' \sin 2\Delta\phi)\rho_{22} \\
 \rho'_{22} &= [(5 - 3 \cos 2\Delta\phi) \cos^2 \theta' + 2 \sin^2 \theta']\rho_{11} \\
 &\quad + [(5 + 3 \cos 2\Delta\phi) \cos^2 \theta \cos^2 \theta' + 2 \cos^2 \theta \sin^2 \theta' \\
 &\quad + 12 \cos \Delta\phi \cos \theta' \cos \theta \sin \theta \sin \theta' + 2 \cos^2 \theta' \sin^2 \theta + 8 \sin^2 \theta \sin^2 \theta']\rho_{22} \\
 &\quad + (6 \sin 2\Delta\phi \cos \theta \cos^2 \theta' + 2 \sin \Delta\phi \cos \theta' \sin \theta \sin \theta')\rho_{12}.
 \end{aligned} \tag{5}$$

When the scattering is resonant with the level  $P_{\frac{1}{2}}$ , then the scattered radiation is characterized with the isotropic angular distribution and hence completely unpolarized. Therefore, the density matrix is constant and  $\frac{1}{2}$  times the identity matrix irrespective of the incident and outgoing wavevectors.

The density matrix elements associated with the outgoing photon given in Eqs. (3-5) are normalized by the unit trace condition. It is readily verified that a  $90^\circ$  scattering of a completely unpolarized incident photon yields 100 percent polarization in the case of a wing scattering and the degree of polarization in the case of a resonant scattering between  $S_{\frac{1}{2}} \rightarrow P_{\frac{3}{2}}$  becomes  $\frac{3}{7}$  (e.g. Chandrasekhar (1960); Lee et al. (1994)).

In Figure 2 we compare the results obtained by using the accelerated code with those calculated by using the original code in our previous works. Here we set the temperature of the scattering media to be  $T = 10$  K or  $a = 1.47 \times 10^{-2}$ , and the photon source is located at the origin of the central plane of the slab, which is the same configuration to the midplane sources by symmetry. In the figure the solid lines stand for those results without the accelerating scheme, and the dashed lines represent the results using the modified code with  $x_c = 1$ . Notable deviation between the two results is seen for  $a\tau_0 \leq 1.47 \times 10^2$  or  $a\tilde{\tau}_0 \leq 2.6 \times 10^2$ . Here  $\tilde{\tau}_0$  is the line-center optical depth defined in terms of the normalized Voigt function in the previous researches (Adams 1972; Neufeld 1990), where  $\tilde{\tau}_0 = \sqrt{\pi}\tau_0$ .

The original code can be regarded as a special case of the accelerated code when  $x_c \rightarrow 0$ . In order to check this, we calculate the emergent profile for the smaller core-wing boundary frequency,  $x_c$ . For the case with  $\tau_0 = 10^3$ , we show our result with  $x_c = 0.6$  by the dotted line in Figure 2. Note that the dashed line for  $\tau_0 = 10^3$  is obtained for  $x_c = 1$ . In the figure we confirm that the emergent profile converges to that from the original code as  $x_c \rightarrow 0$ . It is clear that the accelerated code is much more efficient than the original code, and it gives the correct results.

### 3. Line Transfer in Extremely Thick Media

#### 3.1. Emergent Profiles

In this subsection, we compare our results with analytic solutions and check the validity of our accelerating scheme. In extremely thick media with  $a\tau_0 > 10^3$ , wing scatterings dominate the line transfer in space and the Voigt function  $H(x, a)$  can be approximated by

$$H(x, a) \simeq \frac{a}{\sqrt{\pi}x^2}, \quad (6)$$

where the optical depth at a frequency shift  $x$  is given by  $\tau_x = \tau_0 H(a, x)$ . Adams (1972); Harrington (1973); Neufeld (1990) introduced the diffusion approximation according to which the Ly $\alpha$  photons transfer in space only by wing scatterings, and the distance traversed per scattering is described by Eq. (6). Neufeld (1990) derived an analytic solution for the extremely thick media,

$$J(\pm\tau_0, x) = \frac{\sqrt{6}}{24} \frac{x^2}{a\tau_0} \frac{1}{\cosh[(\pi^4/54)^{1/2}(|x^3|/a\tau_0)]}. \quad (7)$$

We perform Monte Carlo calculations for a monochromatic source with its input frequency  $x_0 = 0$ . We simulate several cases with different  $a\tau_0$  values so that both moderately thick and extremely thick cases are included in the computations. In each case, the source is located at the midplane of a static neutral slab.

First, we set the temperature of the scattering medium to be  $T = 10$  K, which corresponds to  $a = 1.49 \times 10^{-2}$ . The relevant situation for this case may be found in the later evolutionary epoch of starburst galaxies, when the cold supershell with large H I column density expands very slowly. The column density ( $N_{\text{HI}}$ ) of normal galaxies and dwarf galaxies ranges  $N_{\text{HI}} = 10^{19} - 10^{22} \text{ cm}^{-2}$ , which corresponds to the Ly $\alpha$  line-center optical depth  $\tau_0 = 10^6 - 10^9$ . The line-center optical depth is related to the H I column density  $N_{\text{HI}}$  via

$$\tau_0 \equiv 1.41 T_4^{-1/2} \left[ \frac{N_{\text{HI}}}{10^{13} \text{ cm}^{-2}} \right], \quad (8)$$

where  $T_4 = T/10^4\text{K}$  and  $T$  is the temperature of the scattering medium.

Here we choose  $\tau_0 = 10^3, 10^4, 10^5, 10^6, 10^7$  or  $a\tau_0 = 1.49 \times 10, 1.49 \times 10^2, 1.49 \times 10^3, 1.49 \times 10^4, 1.49 \times 10^5$ . We note that these are transformed respectively into  $a\tilde{\tau}_0 = 2.64 \times 10, 2.64 \times 10^2, 2.64 \times 10^3, \text{ and } 2.64 \times 10^4$ .

Our results are shown in Figure 3a and Figure 3b. We see that the profiles of our Monte Carlo results are in good agreement with the analytic solutions for  $a\tau_0 \geq 10^3$ . For  $\tau_0 = 10^3$ , we also show the emergent profile for the case of  $x_c = 0.6$  which is closer to the result of original code in Ahn et al. (2000, 2001). We see that it also shows deviation from the analytic solution derived by Neufeld (1990), which is expected due to the invalidity of diffusion approximation for  $a\tau_0 < 10^3$ . We conclude that our accelerating scheme is valid for the various range of optical depths.

Next, we perform Monte Carlo calculations for hotter media, whose Voigt parameter is given by  $a = 4.71 \times 10^{-4}$  corresponding to  $T = 10^4$  K. We choose  $\tau_0 = 10^6, 10^7, 10^8, \text{ and } 10^9$ , which correspond to  $a\tau_0 = 4.71 \times 10^2, 4.71 \times 10^3, 4.71 \times 10^4, \text{ and } 4.71 \times 10^5$ . We note that these are transformed respectively into  $a\tilde{\tau}_0 = 8.35 \times 10^2, 8.35 \times 10^3, 8.35 \times 10^4, \text{ and } 8.35 \times 10^5$ . In Figure 4, we show the results of our accelerated Monte Carlo code and compare them with the analytic solution, Eq. (7). The solid lines represent the results of our Monte Carlo calculations, and the dotted lines do analytic solutions. We see that our numerical results are in very good agreement with analytic solutions for very thick media ( $\tau_0 \geq 10^8$ ). In extremely thick media, we can safely assume that only wing scatterings contribute to the spatial transfer of Ly $\alpha$  photons, and so our accelerated code can describe the line transfer process very well.

Third, we also perform calculations for sources uniformly distributed along the vertical direction of the slab. The relevant application for this case can be found in the giant H II region, where the Ly $\alpha$  sources and the scattering media may be mixed together. We assume that the typical temperature of H II region is  $T = 10^4$  K, and that the size of H II region is kpc scale. In this environment the degree of ionization can lead to the volume density of neutral hydrogen  $n_{\text{HI}} = 1 \text{ cm}^{-3}$ . Hence the total column density of the H II region can be  $N_{\text{HI}} \sim 10^{20} \text{ cm}^{-2}$ , which corresponds to the line-center optical depth of  $\tau_0 \sim 10^4 - 10^7$ . In the code, we generate the sources at the location  $(p_x, p_y, p_z) = (0, 0, \tau_s)$ , where  $\tau_s = (2R - 1)\tau_0$  and  $R$  is the uniform random number having range of  $[0, 1]$ .

When photon sources are located near the surface, the optical depth toward the nearest boundary is much less than that toward the midplane of the slab. Hence, we adjust the core-wing boundary frequency ( $x_c$ ) in accordance with the vertical location of photon sources which is denoted by  $p_z$ : we used  $x_c = A(1 - p_z/\tau_0)$ , where  $A$  is a core-wing boundary

frequency in units of thermal velocity for midplane sources. This formula gives correct behaviors for both thin and thick cases. Clearly  $x_c \rightarrow 0$  as  $|p_z| \rightarrow \tau_0$ .

In Figure 5 we show our results only for the extremely thick cases with  $\tau_0 = 10^7, 10^8$  and  $a = 4.71 \times 10^{-4}$ . We note that the results for the moderately thick cases can be found in the previous paper (Ahn et al. 2001). Our results (solid lines) are compared with the analytic solutions (dashed lines). From the analytic solutions for the case of midplane source (Neufeld 1990), we obtain the analytic solutions for the case of distributed sources by convolving the midplane solution, Eq. (7), with the uniform source positions ( $\tau_s$ ),

$$J_d(\pm\tau_0, x) = \int_{-\tau_0}^{\tau_0} J_m(\pm\tau_0, x; \tau_s) \delta(\tau_s) d\tau_s. \quad (9)$$

In the figure we can see that our numerical results agree very well with the analytic ones, and that the peaks are more shifted to the line-center compared to the midplane cases. This is because the sources near the surface contribute to the central part of emergent profiles.

Adams (1972) argued that in extremely thick media with  $a\tau_0 > 10^3$ , the emergent flux depends on the product  $a\tau_0$ , not on the individual parameters. This is evidently seen in Eq. (7), in which  $J(\pm\tau_0, x)$  is dependent upon  $a\tau_0$ . In order to check this fact, we perform Monte Carlo calculations for a few pairs of  $a$  and  $\tau_0$  with common  $a\tau_0$  values. For  $a\tau_0 = 4.71 \times 10^2$  (or  $a\tilde{\tau}_0 = 8.35 \times 10^2$ ), we perform calculations for two pairs; ( $a = 4.71 \times 10^{-4}$ ,  $\tau_0 = 10^6$ ) and ( $a = 4.71 \times 10^{-2}$ ,  $\tau_0 = 10^4$ ). For  $a\tau_0 = 4.71 \times 10^3$  (or  $a\tilde{\tau}_0 = 8.35 \times 10^2$ ), we choose ( $a = 4.71 \times 10^{-4}$ ,  $\tau_0 = 10^7$ ) and ( $a = 4.71 \times 10^{-2}$ ,  $\tau_0 = 10^5$ ). The other pair is ( $a = 4.71 \times 10^{-4}$ ,  $\tau_0 = 10^8$ ) and ( $a = 4.71 \times 10^{-2}$ ,  $\tau_0 = 10^6$ ), which have  $a\tau_0 = 4.71 \times 10^4$ . Our results are shown in Figure 6, where we see that, for the extremely thick cases  $a\tau_0 \geq 10^3$ , the line profiles for each pair with the same  $a\tau_0$  agree very well with each other. Thus we confirm that our code reproduces the results in Adams (1972) very well.

Finally, we also consider the radiative transfer of continuum photons near  $\text{Ly}\alpha$ . We simply assume that an input spectrum is flat. In Figure 7 we show our results for  $\tau_0 = 10^4, 10^5, 10^6, 10^7$  fixing  $a = 1.49 \times 10^{-2}$ , where symmetric double peaks and one absorption trough at the line-center are seen. The absorption trough broadens as  $\tau_0$  gets larger. We show the wavelength ( $\lambda$ ) in units of  $\text{\AA}$  on the top edge of the figure, which is scaled by  $\lambda \propto T^{1/2}$ . Here  $T$  is the temperature of the scattering medium. Note again that the spectra are symmetric relative to the line-center.

### 3.2. Limb brightening and darkening

In this subsection we consider the directionality of emergent Ly $\alpha$  photons. In the Monte Carlo code we collect emerging photons with the directional information into the equally spaced bins in  $\mu \equiv \cos\theta$  where  $\theta$  is the angle between the normal direction of the slab and the wavevector of the photons. Since the number of photons along  $\mu$  is proportional to  $I(\mu)\cos\theta d\Omega$ , where  $\Omega$  is the solid angle, we obtain the intensity  $I(\mu)$  by dividing the number of photons by  $\mu$ . We call the function  $I(\mu)$  the ‘directionality’. This definition of directionality is different from that used by Phillips & Mészáros (1986, hereafter PM86), who defined it as the intensity normalized with respect to the intensity normal to the slab.

The results are shown in Figure 8. The curves for  $a\tau_0 \leq 10^3$  are nearly isotropic, because most Ly $\alpha$  photons escape from the medium by single longest flights: each Ly $\alpha$  photon is scattered locally near the source and becomes a wing photon by frequency diffusion, when the medium gets transparent. Therefore, a large number of local scatterings isotropize the radiation field, which is characterized by no or (at least a negligible) polarization.

As  $\tau_0 > 10^3$ , the directionality gradually converges to that of the Thomson-scattered radiation emergent from a Thomson-thick electron medium represented by the thick solid line. This Thomson limit was obtained by Chandrasekhar (1960) and was confirmed numerically by PM86. PM86 also provided the results for optically thin as well as optically thick cases. Therefore, we compare our results with those from the radiative transfer in a pure electron scattering medium, because Thomson scattering shares the same Rayleigh phase function as Ly $\alpha$  wing scattering.

It is convenient to consider the effective wing optical depth,  $\tau_w$ , which is the optical depth at the effective frequency of emergent photons,  $x_s = (a\tau_0)^{1/3}$ . From Eq. (6) we can see that

$$\tau_w = \frac{1}{\sqrt{\pi}}(a\tau_0)^{1/3} = \frac{1}{\sqrt{\pi}}x_s. \quad (10)$$

We compare this optical depth with the optical depth for the Thomson scattering defined by  $\tau_e = \sigma_T N_e$ , where  $\sigma_T = 0.665 \times 10^{-24}$  cm<sup>2</sup> is the Thomson scattering cross section, and  $N_e$  is the electron column density.

When  $a\tau_0$  is small, after a large number of local resonant scatterings, a Ly $\alpha$  photon becomes a wing photons due to the scattering with a fast moving hydrogen atom. Now, for this wing photon the slab is a transparent medium, especially along the normal direction and escape to this direction occurs without subsequent scatterings. However, to the grazing direction, because of simple geometrical considerations, there can be a significant probability of further wing scatterings before escape. Therefore, the situation becomes quite similar to the electron scattering in a plane-parallel slab that is quite thin and illuminated from the

other side. Limb brightening is a natural consequence because we see more sources in the grazing direction, as is shown in Figure 8.

For the extremely thick cases with  $a\tau_0 > 10^3$ , the effective wing optical depth is estimated to be  $\tau_w > 6$  by Eq. (10). This corresponds to the result of the Thomson scattered radiation in an electron cloud with its optical depth  $\tau_e > 6$ . This limiting behavior of the directionality may be summarized as

$$\frac{I(\mu)}{I(\mu = 1)} \simeq \frac{1}{3}(1 + 2\mu), \quad (11)$$

which is an approximate relation proposed by PM86 for the numerical solution introduced in the Table XXIV of Chandrasekhar (1960). This is shown by a thick solid line in Figure 8. We see that the directionality of Ly $\alpha$ , being transferred in an extremely thick hydrogen medium, converges to that for the case of optically thick electron cloud. In this optical depth regime, the optical depth for Ly $\alpha$  wing photons becomes large, and the photons spatially transfer in the medium by random walks. Hence, the escape of photons occurs preferentially to the normal to the slab, where the opacity is relatively small. We regard this phenomenon as a limb darkening, which was also called a ‘beaming’ by PM86.

In an extremely thick medium, Ly $\alpha$  photons experience a number of successive wing scatterings just before their escape from the medium during their single longest excursion. How many times do the photons experience the successive wing scatterings just before escape? According to Adams (1972), in an extremely thick medium with an isotropic Ly $\alpha$  source located at the midplane, photons acquire a typical frequency shift  $x_s = (a\tau_0)^{1/3}$  during excursions (see also section 2 of this paper). In an extremely thick medium, the spatial transfer of Ly $\alpha$  photons occurs during a series of wing scatterings, and so we can approximate the spatial transfer by random walks. Thus from Eq. (10) we can estimate the mean number of successive wing scatterings just before escape ( $\langle N_w \rangle$ ) by

$$\langle N_w \rangle = \tau_w^2 = \frac{1}{\pi}(a\tau_0)^{2/3} \quad (12)$$

or

$$\log_{10}\langle N_w \rangle = \frac{2}{3}\log_{10}(a\tau_0) - 0.497. \quad (13)$$

In the accelerated Monte Carlo calculations we count the number of wing scatterings just before escape, and compare the result with the above relationship. In the upper panel of Figure 9 we show the spectral distribution of the number of wing scatterings just before escape. We can see that the photons emerging with larger frequency shift have been experienced more wing scatterings just before escape than those with smaller frequency shift.

In order to check the relationship of Eq. (13), we show in Figure 10 the graph of  $\log_{10}\langle N_w \rangle$  vs.  $\log_{10} a\tau_0$ , where  $\langle N_w \rangle$  is the value averaged over frequency, and  $a\tau_0$  represents the importance of wing scatterings in Ly $\alpha$  line transfer. Here the number of photons for each point is 4000, and the error in  $N_w$  is the flux weighted Poisson error. The least square fitting gives us the following relationship,

$$\log_{10}\langle N_w \rangle = (0.674 \pm 0.010) \log_{10} a\tau_0 - (0.552 \pm 0.042). \quad (14)$$

We see that the power and the coefficient in Eqs. (13) and Eq. (14) are in good agreement with each other.

#### 4. Discussion

We have investigated the Ly $\alpha$  line transfer in extremely thick, dustless, uniform, and static media. In order to reduce the calculation speed, we developed an accelerating scheme for our previous Monte Carlo code, in which we skip an extremely large number of core scatterings that may occur during the line transfer. The code also deals with the angular redistribution accurately by using the density matrix formalism where the phase functions calculated in a manner faithful to the atomic physics. The modified code passes the requirement in both efficiency and accuracy when calculating the Ly $\alpha$  line profiles emergent from extremely thick media. We checked that the line profile is dependent only upon  $a\tau_0$ , which was argued by Adams (1972). With the code we obtained solutions for both the midplane source and the uniformly distributed sources, both of which show excellent agreement with the analytic solutions derived by Neufeld (1990). In the latter case, the peaks tend to shift toward the line-center due to the sources located near the slab surface. We also presented our results on the radiative transfer of continuum photons near Ly $\alpha$ , and the emergent spectra show the double peaks and the broad absorption at the line-center. However, it is natural to think that dust extinction will destroy a significant fraction of photons forming the double peaks, and eventually a broad absorption trough will form.

We also examined the directionality of emergent Ly $\alpha$  photons. When the medium is slightly thick with  $a\tau_0 \ll 10^3$ , we observe a limb brightening effect, because the slab becomes transparent to wing photons. As  $a\tau_0$  increase, the directionality eventually converges to that of the Thomson scattered radiation in a thick electron cloud which was investigated by Chandrasekhar (1960). The limiting behavior of the curves is the beaming of Ly $\alpha$  photons into the direction normal to the slab. In short, the Ly $\alpha$  emission from the star-forming regions that are surrounded by scattering neutral media shows the limb brightening when  $a\tau_0 \ll 10^3$ , and the limb darkening when  $a\tau_0 > 10^3$ . These facts can be physically explained,

since both the Ly $\alpha$  scattering by neutral hydrogen at wings and the Thomson scattering in an electron cloud have the same Rayleigh phase function.

We also counted the mean number of successive wing scatterings just before escape, which is denoted by  $\langle N_w \rangle$ , and by Monte Carlo calculations we confirmed the relationship  $\langle N_w \rangle = \frac{1}{\pi}(a\tau_0)^{2/3}$ , which is derived from the diffusion approximation.

In conclusion, it is important to consider the quantum mechanical properties of Ly $\alpha$  scatterings and the exact transfer processes, and our accelerated Monte Carlo code can afford those requirements as well as the computing time.

Our works can be applied to local and distant starburst galaxies. Approximately half of their Ly $\alpha$  lines show broad absorption troughs in the Lorentzian wings. These absorption troughs are believed to be formed by optically thick, static H I media with some amount of dust. However, the media in this study have been assumed to be dustless, which is unrealistic for almost all situations. Hence, we will take dust effects into account in the future works. Moreover, the emergent profiles are also influenced by the physical quantities such as porosity of dust and homogeneity of the medium as well as dust abundance and H I column density, so that we are now undertaking investigations about the effects of these components on the line formation.

Another half of the starburst galaxies, either nearby or remote, show P-Cygni type Ly $\alpha$  emission. As Kunth et al. (1998) suggested, expanding media around the star-forming regions play an important role in avoiding the destruction of Ly $\alpha$  photons by dust and forming the P-Cygni type Ly $\alpha$  profiles. When we calculated the Ly $\alpha$  line formation in an expanding medium, it is difficult to deal with the back-scattered photons. We have been investigating this topic by applying the formalism developed in this paper, and the results will be reported in another paper.

In conclusion, Ly $\alpha$  from starburst galaxies bears important and useful information on the physical environment of those systems including the kinematics, H I column density, abundance and porosity of dust in the surrounding media of the star-forming regions in those galaxies. Being very luminous in addition to being sensitive to many physical quantities, Ly $\alpha$  can be easily observed by using the modern observational technology.

This work was achieved as a part of doctoral dissertation in the School of Earth and Environmental Sciences of Seoul National University financially supported by Brain Korea 21 of the Korean Ministry of Education. SHA and HML appreciate the support. Also this work is completed with the financial support of the Korea Institute for Advanced Study, which is pleasantly acknowledged.

## REFERENCES

- Adams, T. 1972, ApJ, 174, 439
- Ahn, S. -H., Lee, H. -W., & Lee, H. M. 2000, J. Korean Astron. Soc., 33, 29
- Ahn, S. -H., Lee, H. -W., & Lee, H. M. 2001, ApJ, 554, 1
- Avery, L. W., & House, L. L. 1968, ApJ, 152, 493
- Chandrasekhar, S. 1960, Radiative Transfer (New York:Dover)
- Condon, E. U. & Shortley, G. H. 1951, The Theory of Atomic Spectra. Cambridge Univ. Press, Cambridge
- Gould, A., & Weinberg, D. H. 1996, ApJ, 468, 462
- Harrington, J. P. 1973, MNRAS, 162, 43
- Kunth, D., Mas-Hesse, J. M., Terlevich, E., Terlevich, R., Lequeux, J., & Fall, S. M. 1998, A&A, 334, 11
- Lee, H. -W., & Ahn, S. -H. 1998, ApJ, 504, 61
- Lee, H. -W., Blandford, R. D., & Western, L. 1994, MNRAS, 267, 303
- Legrand, F., Kunth, D., Mas-Hesse, J.M., & Lequeux, J. 1997, A&A, 326, 929
- Meier, R. R., & Lee, J. -S. 1981, ApJ, 250, 376
- Neufeld, D. A. 1990, ApJ, 350, 216
- Phillips, K. C., & Mészáros, P. 1986, ApJ, 310, 284 (PM86)
- Steidel, C. C., Giavalisco, M., Pettini, M., Dickinson, M., & Adelberger, K. L. 1996, ApJ, 462, 17
- Steidel, C. C., Adelberger, K. L., Giavalisco, M., Dickinson, M., & Pettini, M. 1999, ApJ, 519, 1
- Stenflo, J. O. 1980, A&A, 1984, 68
- Tenorio-Tagle G., Silich S. A., Kunth D., Terlevich E., & Terlevich R. 1999, MNRAS, 309, 332

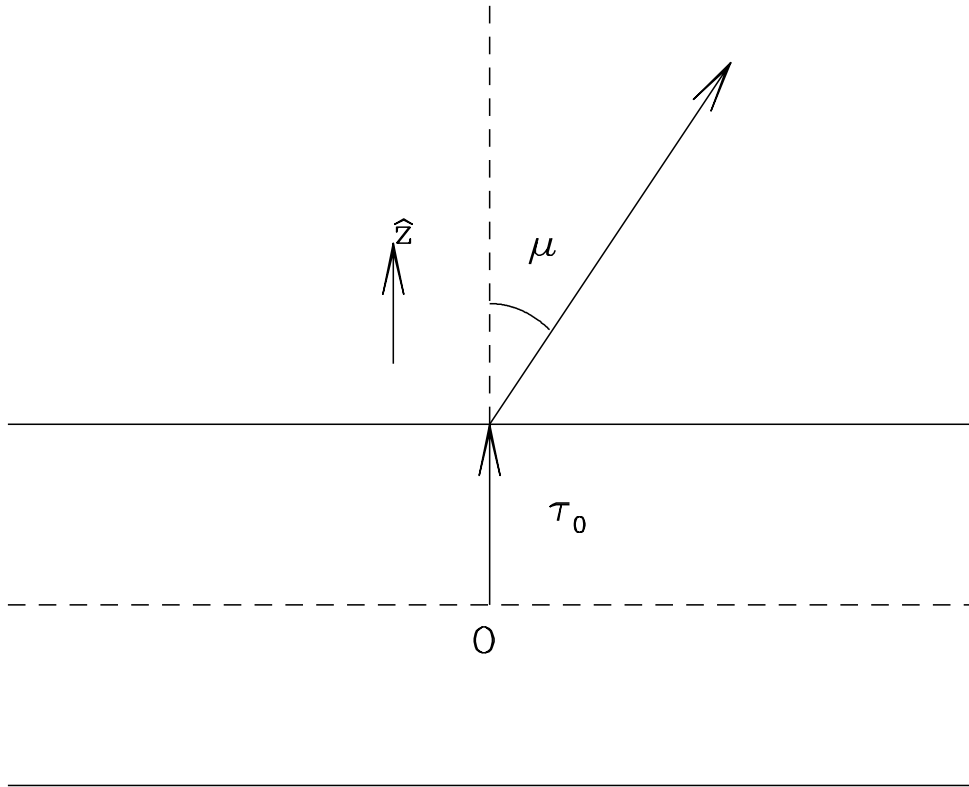


Fig. 1.— Configuration studied in this work. We consider the static and uniform slab. We also consider two types of source distribution: in one type the Ly $\alpha$  source is located at the origin denoted in the figure by  $O$ , and in the other they are uniformly scattered along z-axis. The vertical thickness of the slab is  $2\tau_0$ , and we define  $\mu$  as the cosine of the angle between the wave vector of the emergent photon and the slab normal.

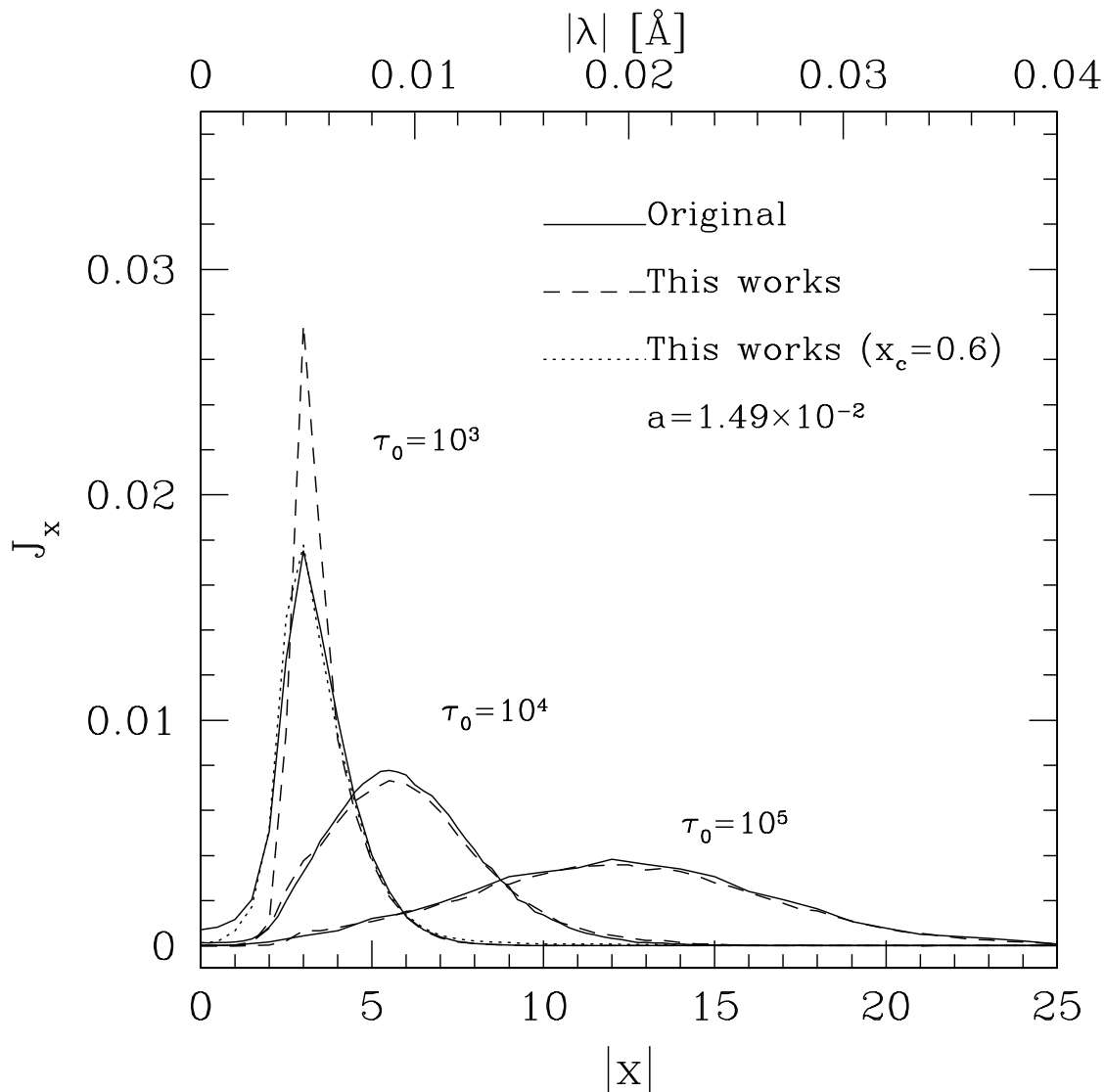


Fig. 2.— Comparisons between the results of the original code (solid line) and those of the code with the accelerating scheme (dashed line). The bottom horizontal axis represents frequency shift  $x$  in units of the thermal width, and the top horizontal axis represents wavelength for  $T = 10\text{K}$ . Comparisons were made for the case of midplane sources radiating monochromatic Ly $\alpha$  photons with  $x_0 = 0$ . The dotted line represents the result for a small core-wing boundary frequency,  $x_c$ .

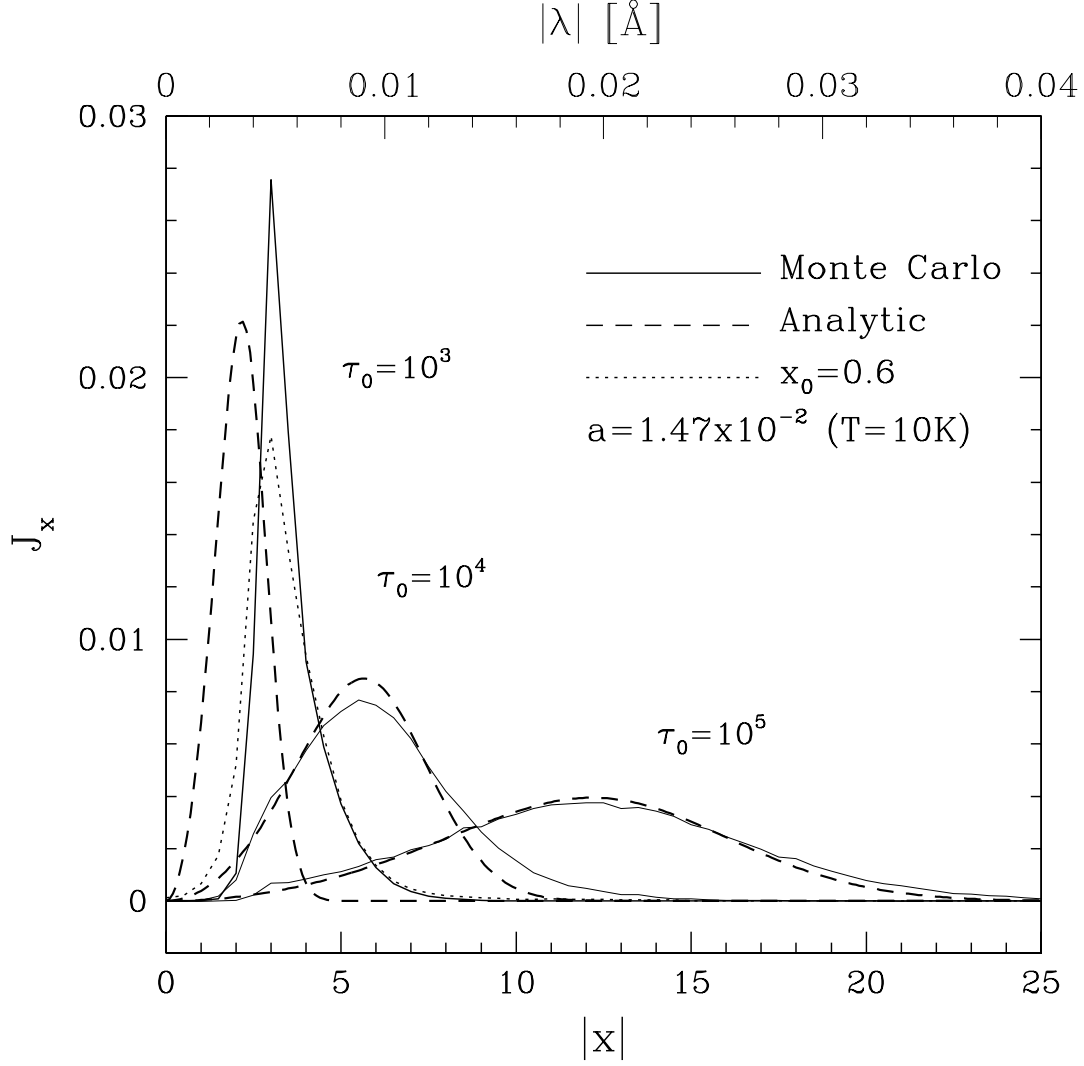


Fig. 3.— Ly $\alpha$  profiles emerging from thick media of different  $\tau_0$ 's, where we fix  $a = 1.49 \times 10^{-2}$  or  $T = 10$  K. The bottom horizontal axis represents frequency in units of the thermal width, and the top horizontal axis represents wavelength shift for  $T = 10$  K. Here the solid lines stand for results of our Monte Carlo calculations, and the dashed lines for the analytic solutions given by Neufeld (1990). The total flux of the line is normalized to  $1/4\pi$  in accordance with Neufeld's normalization. We note that the profiles are symmetric about the origin,  $x = 0$ .

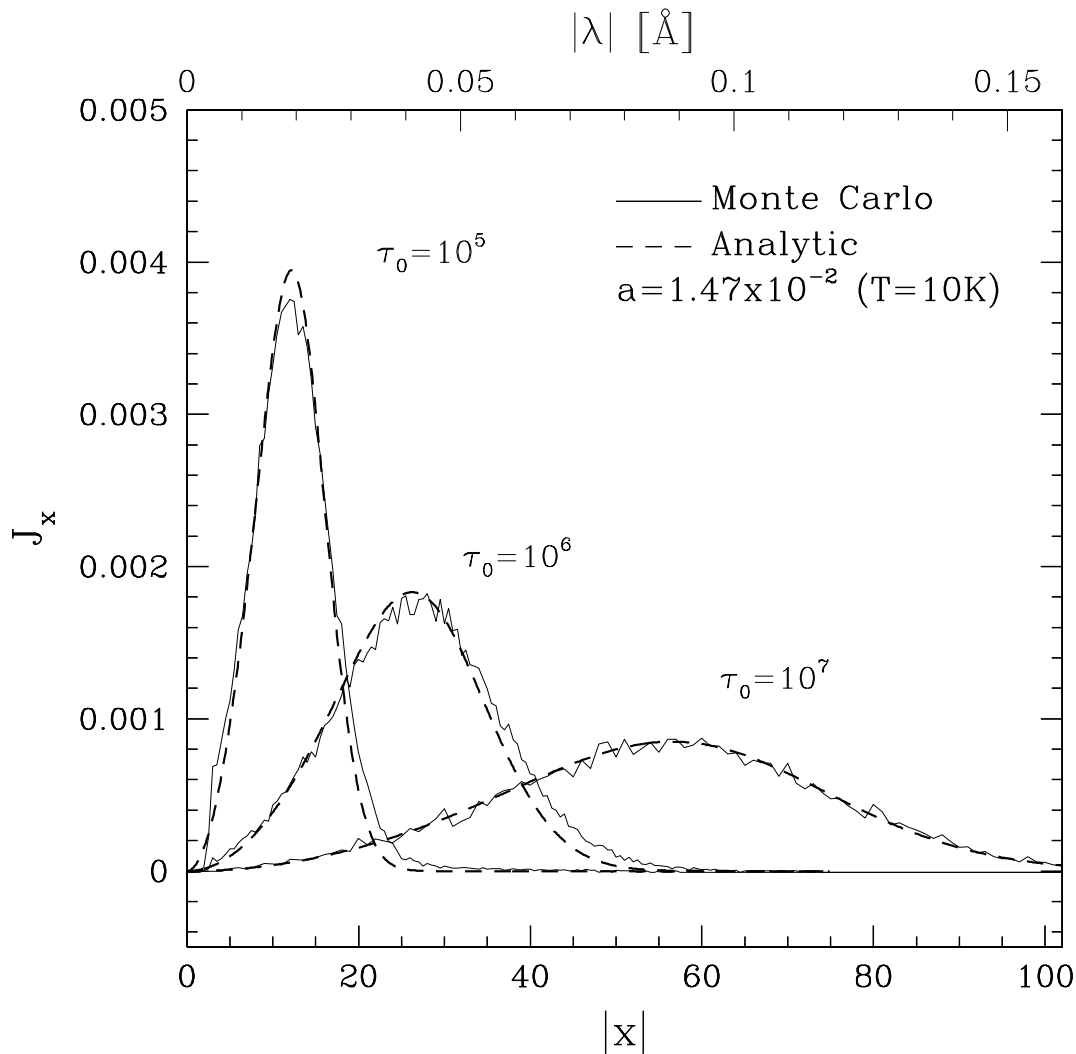


Fig. 4.— Ly $\alpha$  profiles emerging from extremely thick media with different  $\tau_0$ 's and a common Voigt parameter  $a = 1.49 \times 10^{-2}$  corresponding to  $T = 10$  K. Here the solid lines stand for the results of our Monte Carlo calculations, and the dashed lines for the analytic solutions given by Neufeld (1990). Here horizontal axis represents frequency shift  $x$  in units of the thermal Doppler width, and the total flux of the line is normalized to  $1/4\pi$  in accordance with Neufeld's normalization. Note that the profiles are symmetric about the origin,  $x = 0$ .

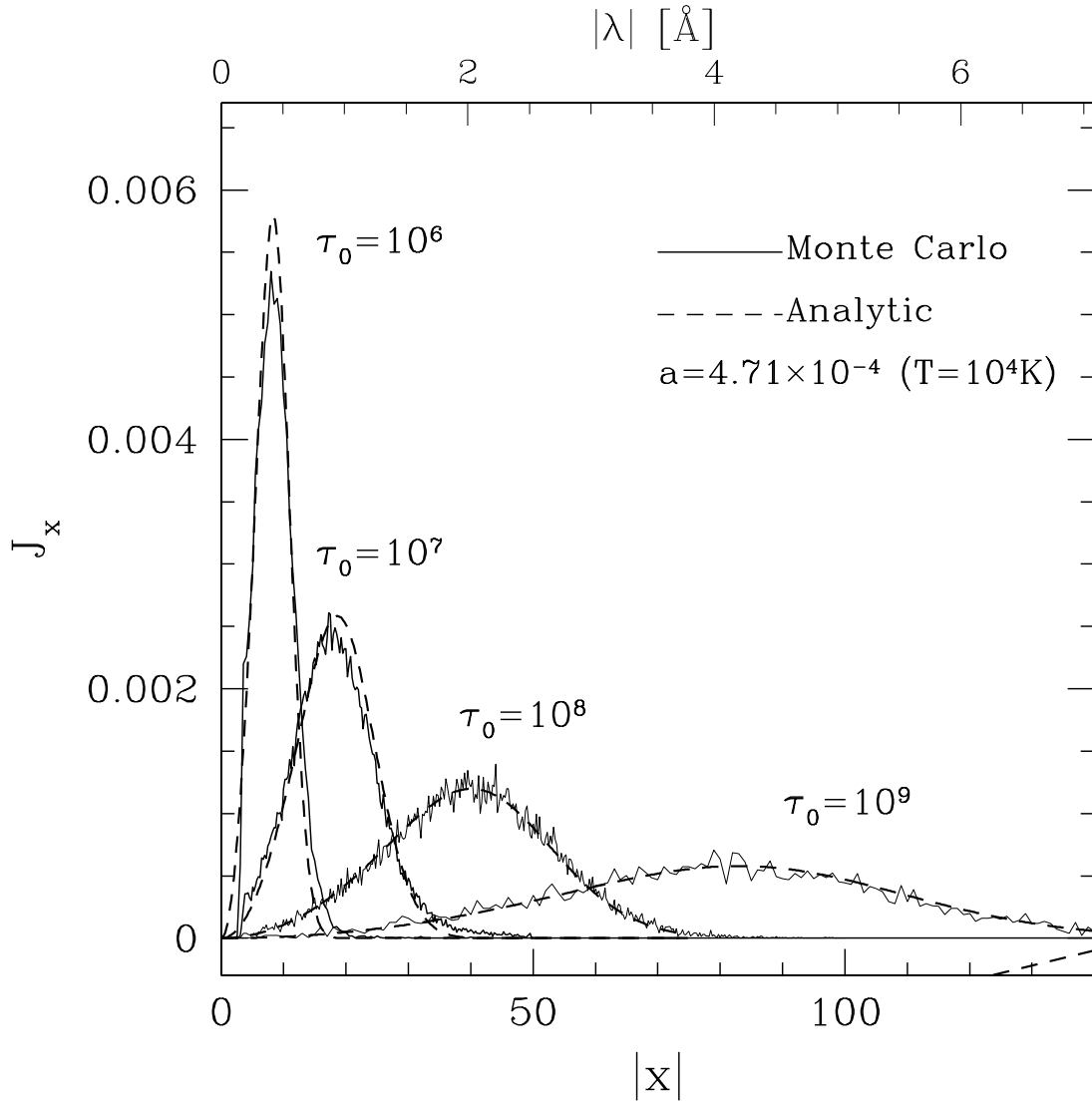


Fig. 5.— Our emergent profiles (solid lines) are compared with Neufeld’s analytic solution (dotted lines).

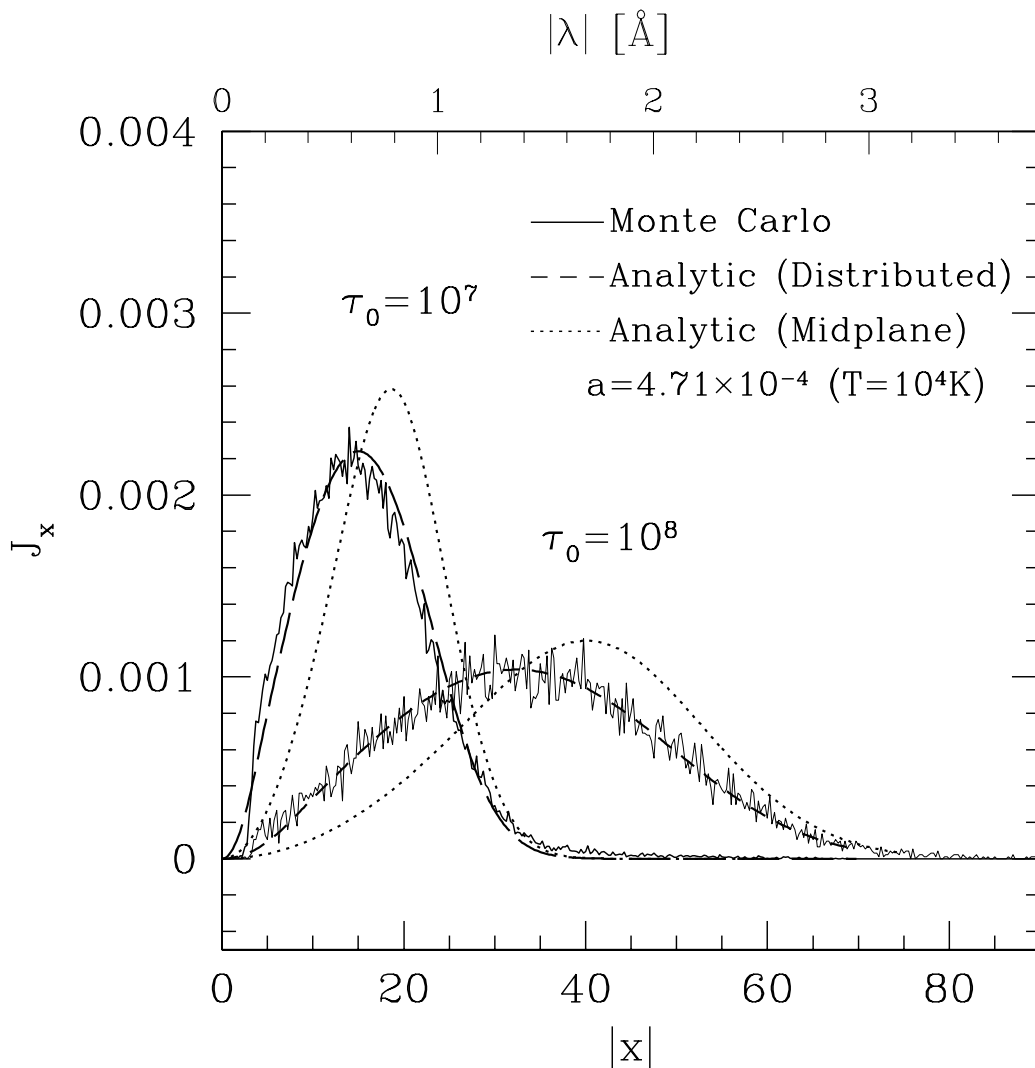


Fig. 6.— Emergent profiles for the cases of distributed sources. Comparing with the mid-plane solutions of the same  $a$  and  $\tau_0$  (dotted lines), their peaks are shifted to the line-center. Here solid lines represent our Monte Carlo results, and the dashed lines do the analytic solutions obtained by convolving Neufeld’s solution.

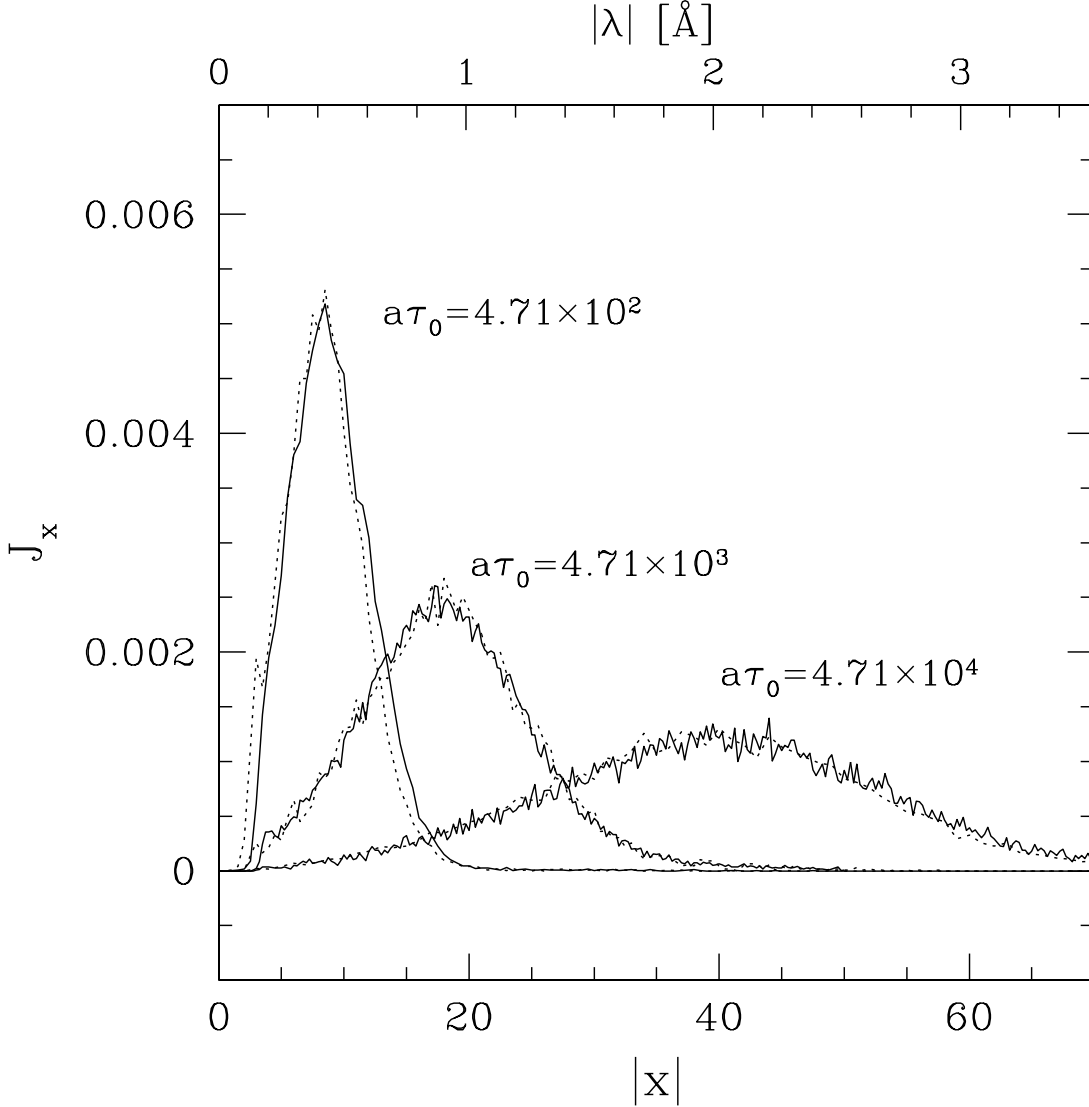


Fig. 7.— Emergent profiles of a few pairs of Monte Carlo simulations which have the common  $a\tau_0$  values. The pair of physical parameters in the calculations are listed in the text. We see that the cases with the same  $a\tau_0$  show the same emergent profiles. Note that the profile is symmetric with respect to the origin  $x = 0$ . On the top horizontal axis is shown the wavelength ( $\lambda$ ) in units of  $\text{\AA}$ , which scales  $\lambda \propto T^{1/2}$ . Here  $T$  is the temperature of the scattering medium, and set to be  $T = 10^4\text{K}$  or  $a = 4.71 \times 10^{-4}$ . For  $T = 10\text{K}$  or  $a = 1.49 \times 10^{-2}$ , the wavelength scales are smaller by a factor of  $\sqrt{1000} = 31.6$ , because  $\Delta\nu_D \propto T^{1/2}$ .

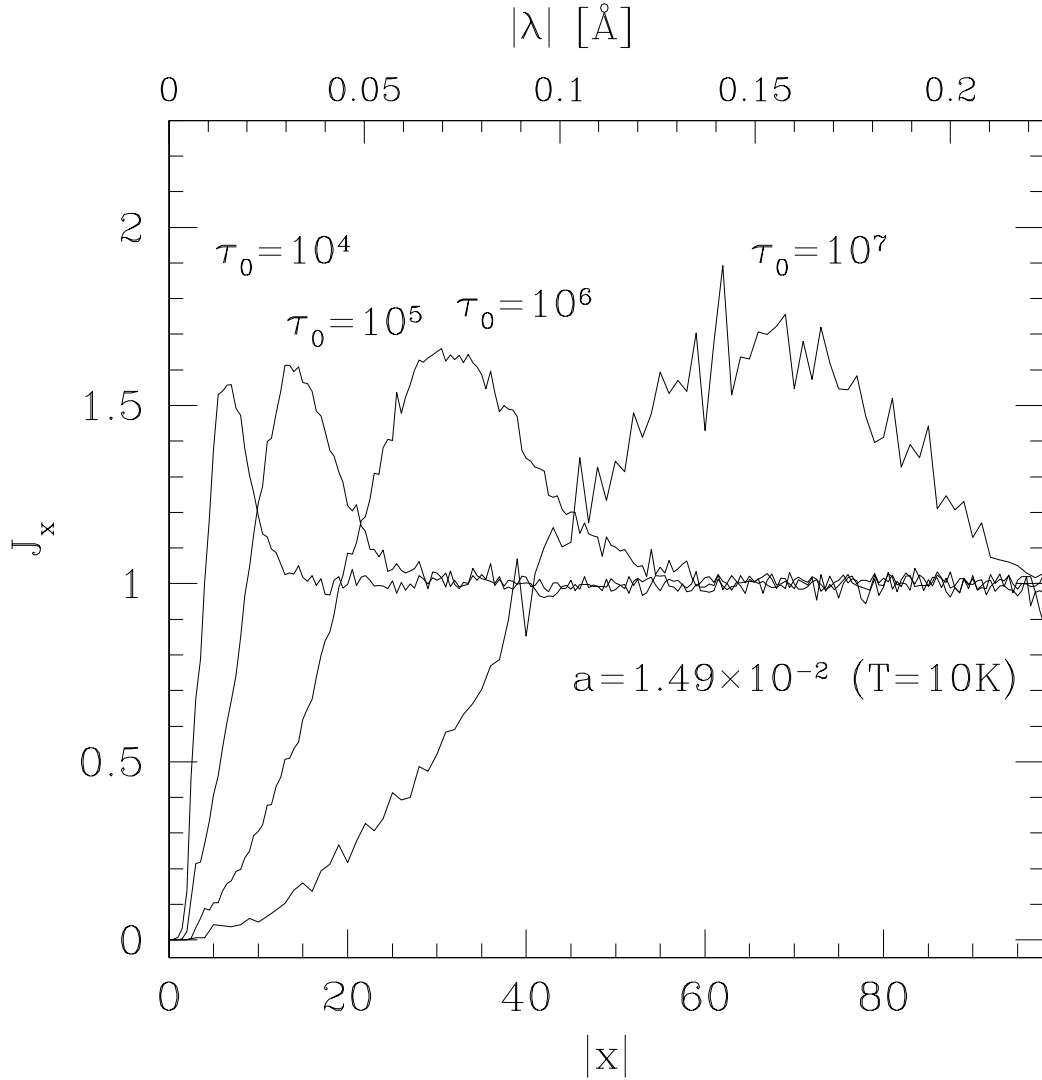


Fig. 8.— Emergent spectra near Ly $\alpha$  when the continuum source is at the center of the scattering medium. Here  $a = 1.49 \times 10^{-2}$  is assumed, and the spectra are normalized to the continuum level. We also denote the wavelength in Å on the top edge of the figure.

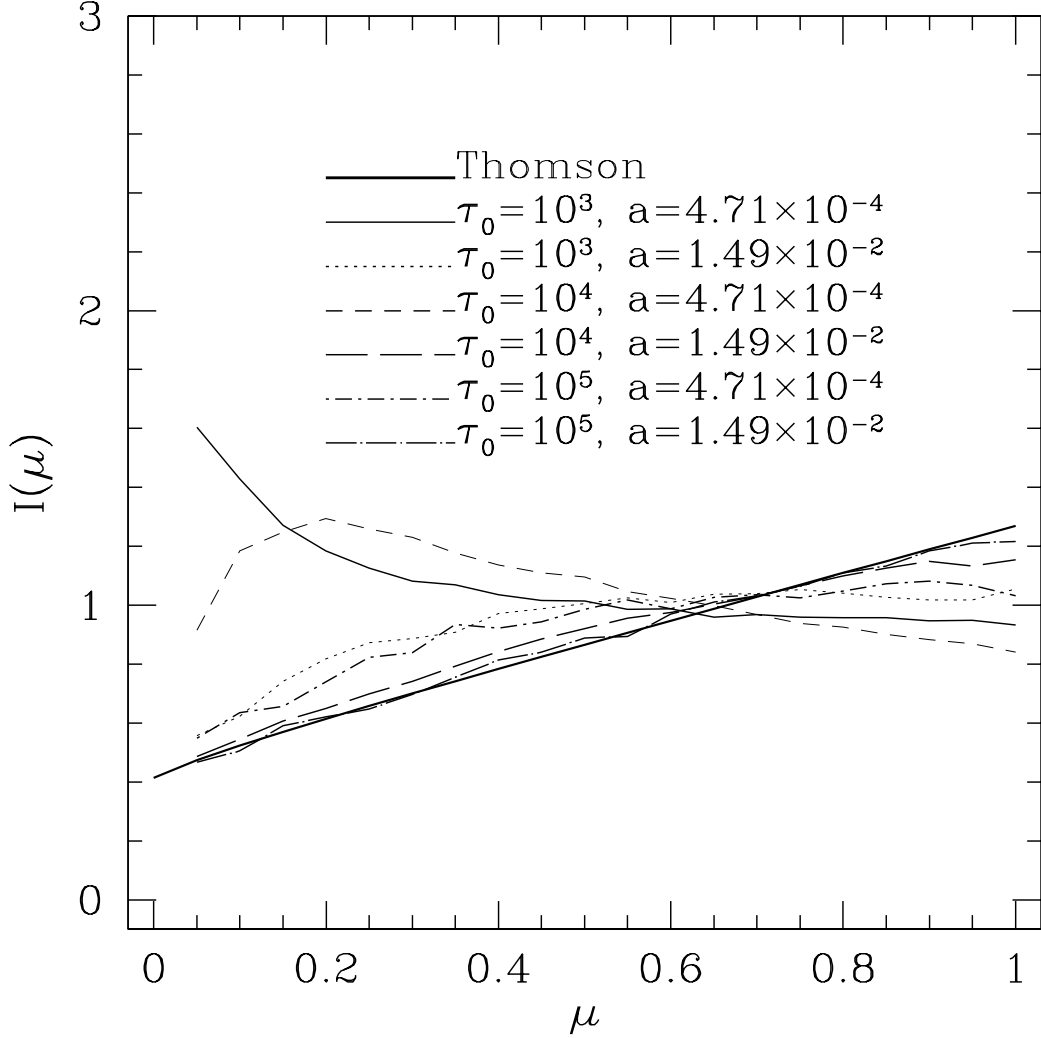


Fig. 9.— Directionality of emergent Ly $\alpha$  photons for various optical depths  $\tau_0$  and Voigt parameters  $a$  of scattering media. We define the directionality by the flux divided by  $\mu$ . The solid thick line represents the limiting behavior of directionality for the Thomson scattered radiation in an opaque electron cloud with the radiation source deep in the cloud. The radiation distribution is almost isotropic when the wing scattering optical depth is small, and converges to take the form of a linear function  $I(\mu) = a + b\mu$ , which is also the limit attained in the very thick Thomson scattering medium obtained by Chandrasekhar (1960).

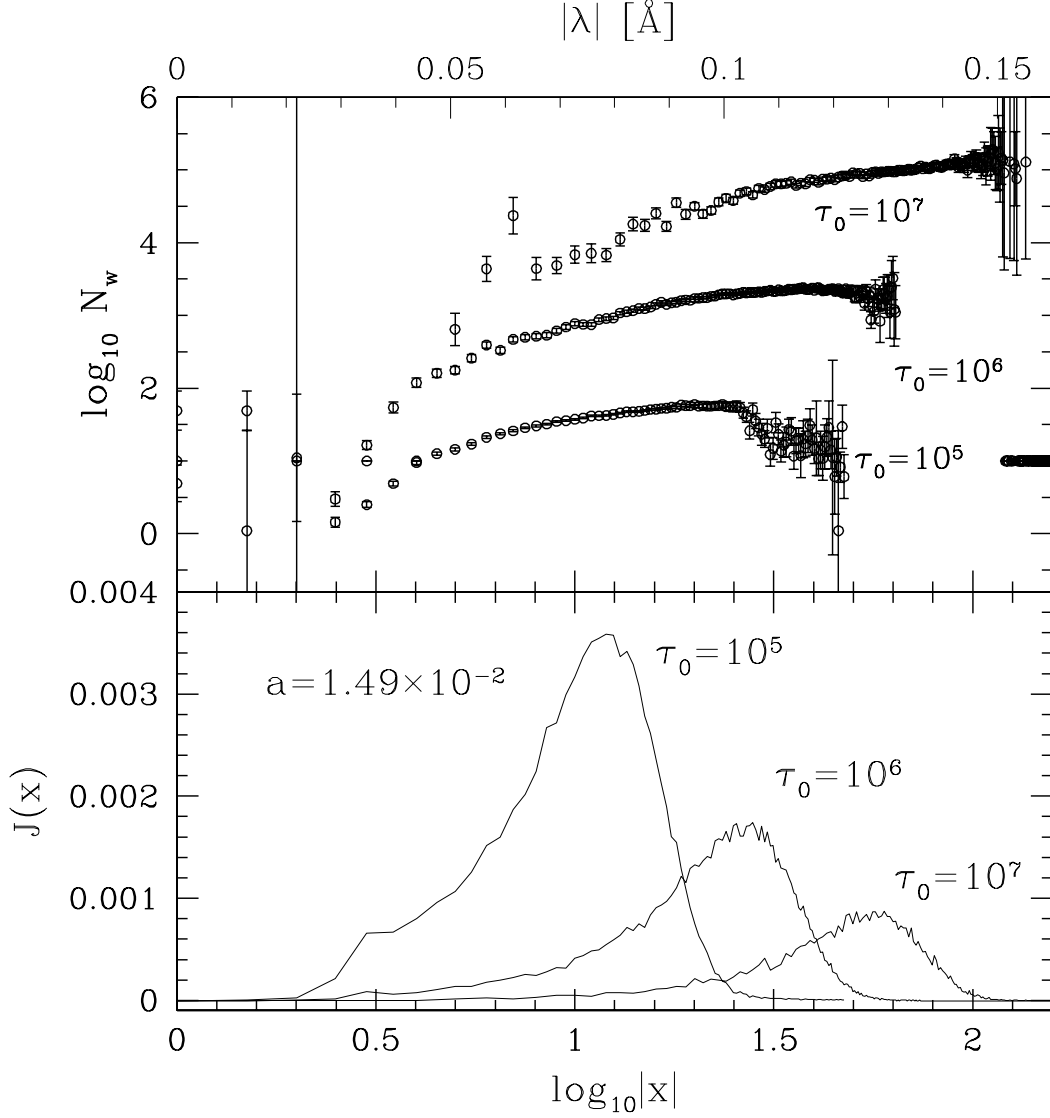


Fig. 10.— Numbers of successive wing scatterings just before escape of Ly $\alpha$  photons,  $N_w$  versus the frequency,  $x$ . The source is located in the midplane of the slab whose temperature is  $T = 10\text{K}$  or  $a = 1.49 \times 10^{-2}$ . The line-center optical depths are  $\tau_0 = 10^5, 10^6, 10^7$ . We show  $N_w$  with the Poisson errors, and for clarity we added one and two to the curves for  $\tau_0 = 10^6$  and  $\tau_0 = 10^7$ , respectively.

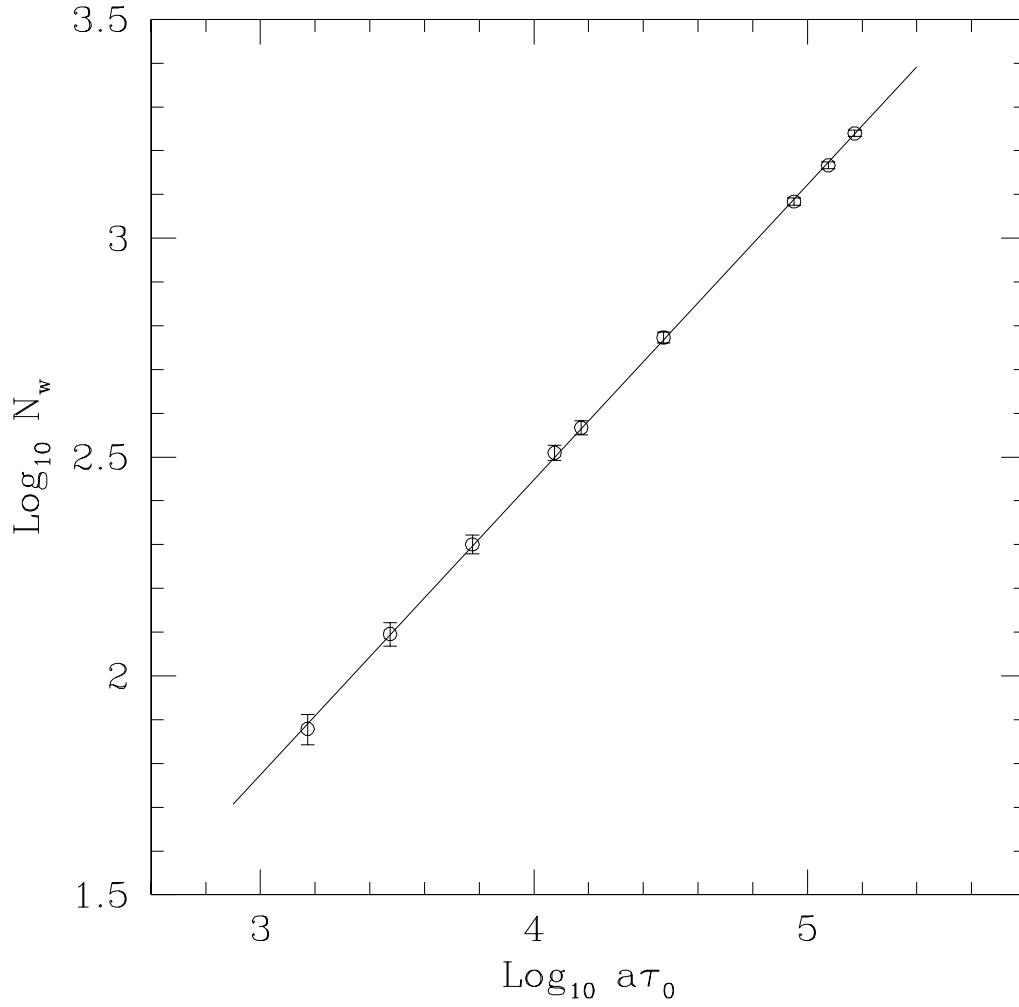


Fig. 11.— The number of a series of wing scatterings just before escape ( $N_w$ ) versus effective optical thickness ( $a\tau_0$ ). Both are presented in logarithmic scales. The error bars are those of flux-weighted errors, and the straight line shows the least square fit.